Saudi Journal of Biological Sciences (2017) **24**, 208–216

King Saud University

Saudi Journal of Biological Sciences

www.ksu.edu.sa
www.sciencedirect.com

ORIGINAL ARTICLE

Extracellular biosynthesis of silver nanoparticles using *Rhizopus stolonifer*

Khalid AbdelRahim [a,b,*], Sabry Younis Mahmoud [c], Ahmed Mohamed Ali [c], Khalid Salmeen Almaary [a], Abd El-Zaher M.A. Mustafa [a,d], Sherif Moussa Husseiny [e]

[a] *Botany and Microbiology Department, College of Science, King Saud University, P.O. Box 2455, Riyadh 11451, Saudi Arabia*
[b] *Botany Department, Faculty of Science, Sohag University, Sohag 82524, Egypt*
[c] *Department of Medical Laboratory Technology, College of Applied Medical Science, University of Dammam, 1704, Hafr Al Batin 319 91, Saudi Arabia*
[d] *Department of Botany, Faculty of Science, Tanta University, Tanta, Egypt*
[e] *Faculty of Women for Art, Science and Education, Ain Shams University, Egypt*

Received 5 December 2015; revised 23 February 2016; accepted 29 February 2016
Available online 10 March 2016

KEYWORDS

Nanoparticles;
Silver;
Rhizopus stolonifer

Abstract Synthesis of silver nanoparticles (AgNPs) has become a necessary field of applied science. Biological method for synthesis of AgNPs by *Rhizopus stolonifer* aqueous mycelial extract was used. The AgNPs were identified by UV–visible spectrometry, X-ray diffraction (XRD), transmission electron microscopy (TEM) and Fourier transform infrared spectrometry (FT-IR). The presence of surface plasmon band around 420 nm indicates AgNPs formation. The characteristic of the AgNPs within the face-centered cubic (fcc) structure are indicated by the peaks of the X-ray diffraction (XRD) pattern corresponding to (111), (200) and (220) planes. Spherical, mono-dispersed and stable AgNPs with diameter around 9.47 nm were prepared and affirmed by high-resolution transmission electron microscopy (HR-TEM). Fourier Transform Infrared (FTIR) shows peaks at 1426 and 1684 cm^{-1} that affirm the presence of coat covering protein the AgNPs which is known as capping proteins. Parameter optimization showed the smallest size of AgNPs (2.86 ± 0.3 nm) was obtained with 10^{-2} M $AgNO_3$ at 40 °C. The present study provides the proof that the molecules within aqueous mycelial extract of *R. stolonifer* facilitate synthesis of AgNPs and highlight on value-added from *R. stolonifer* for cost effectiveness. Also, eco-friendly medical and nanotechnology-based industries could also be provided. Size of prepared AgNPs could be controlled by temperature and $AgNO_3$ concentration. Further studies are required to study effect of

* Corresponding author at: Botany and Microbiology Department, College of Science, King Saud University, P.O. Box 2455, Riyadh 11451, Saudi Arabia. Tel.: +966 0114675818; fax: +966 0114675833.
E-mail address: kabdelraheem@ksu.edu.sa (K. AbdelRahim).

Peer review under responsibility of King Saud University.

Production and hosting by Elsevier

http://dx.doi.org/10.1016/j.sjbs.2016.02.025

more parameters on size and morphology of AgNPs as this will help in the control of large scale production of biogenic AgNPs.

1. Introduction

Nanotechnology is a fast growing branch of science that deals with synthesis and development of varied nanomaterials. Now, various kinds of metal nanomaterials are being prepared by copper, zinc, titanium, magnesium, gold, alginate and silver (Basavaraj et al., 2012). AgNPs became the main focus of intensive research because of their wide selection of applications in areas like catalyst, optics, antimicrobials, and biomaterial production (Qin et al., 2011; Rai et al., 2009; Rao et al., 2000; Zhang et al., 2011; Zhong-jie et al., 2005). Silver nanoparticles showed new or improved properties due to their unique size, morphology, and distribution. At the moment, there's a growing demand to develop eco-friendly nanoparticles using safe chemicals in the synthesis protocol.

Researcher turned to biological system for synthesis of nanoparticles as alternatives to chemical and physical methods. These as a result of several unicellular and multicellular organisms are well-known producing inorganic materials either intra- or extra-cellular (Simkiss and Wilbur, 1989; Mann, 1996). Biosynthesis of nanoparticles such as nanosilver and control in their size composition and mono-disparity are important areas of research in nanoscience, Silver nanoparticles are widely used among all nanomaterials. So biological and biomimetic approaches for biological synthesis of AgNPs are under research. Biomass or extracellular materials from microorganisms like *Fusarium oxysporum*, *Escherichia coli*, *Aspergillus flavus*, licheniformis are used for biotransformation of silver ions to AgNPs (Kim et al., 1998; Cho et al., 2005; Ahmad et al., 2003; Shahverdi et al., 2007). The aim of this study is to biosynthesize AgNPs using fungi *Rhizopus stolonifer* which is a cheap, safe, nonpolluting and acceptable method. Filamentous fungi are more preferred than bacteria and unicellular organisms as they are easy to handle and able to synthesize AgNPs extracellular (Kalishwaralal et al., 2008). Synthesized nanoparticles by fungi are more stable with better mono-disparity (Balaji et al., 2009). In this study we prepared stabilized AgNPs by aqueous extract of *R. stolonifer*, characterized by UV–Visible absorption spectra, XRD, FTIR and confirmed by TEM. Also we investigate effect of temperature and $AgNO_3$ concentration on size of prepared $AgNO_3$.

2. Material methods

2.1. Materials

All used chemicals in present study obtained from Sigma–Aldrich, USA. Fresh deionized water was used during the experimental work.

2.2. R. stolonifer isolation and identification

R. stolonifer was isolated from naturally infected tomato fruits according to Mukherjee et al. (2008). Potato dextrose Agar (PDA) medium supplemented with (30 mg L^{-1}) chloramphenicol to discourage bacterial contamination was prepared routinely and used for fungal isolation. Monosporic cultures were obtained by cultivation of serial dilutions from pure cultures after that individual spores were collected and grown on PDA. Isolates were identified according to their cultural and morphological characteristics based on identification standards (Govindaraju et al., 2010).

2.3. Biosynthesis of silver nanoparticles

Biomass was produced by cultivation of *R. stolonifer* in Malt Glucose peptone (MGYP) broth composed of yeast extract and malt extract 0.3% each, glucose 1%, peptone 0.5%. Culture was incubated at 40 °C on an orbital shaker 180 rpm for 3 days (Balali et al., 1995). Culture was filtered and the resulted biomass was washed extensively by deionized water to get rid of adhered media parts. Mycelia extract was prepared by suspension of fungal biomass in 100 ml deionized water and incubated as described above for 72 h, after that mycelia suspension was filtered using (Whatman paper No. 1). The Resulted filtrate (mycelia extract) was mixed with $AgNO_3$ solution (1 mM $AgNO_3$ final concentration) and incubated on orbital shaker 180 rpm at 40 °C for two days.

2.4. UV–visible spectrometry measurement

Biotransformation of silver ions was monitored by UV–visible spectroscopy measurement of the reaction medium. Three milliliters of supernatant were taken after 6, 12, 24, 36 and 48 h and absorbance was scanned by Labomed, UV–vis double beam (Labomed, Inc, USA) within the wave length ranging from 200 to 600 nm. The absorption of the visible depends directly on color of the chemicals in solution.

2.5. X-ray diffraction (XRD) measurement

XRD technique was used for checking quality of prepared nanoparticles. XRD pattern of drop-coated films of synthesized nanoparticles on glass material was recorded in a wide selection of Bragg angles 2θ at a scanning rate of 20 min^{-1}, using Philips PW 1830 instrument (Philips, Inc, USA) adjusted at 40 kV and 30 mA with metal Cu kα radiation (λ = 1.5405 Å).

2.6. TEM measurements

The morphology and size of AgNPs were determined using TEM by Transferring aliquot of aqueous suspension of AgNPs onto a carbon coated copper grid and allowed to be air dried (Domsch et al., 1993). The grid was then scanned employing a Phillips EM 208S transmission microscope (Philips, Inc, USA) adjusted at 100 kV.

2.7. Fourier rework Infrared (FT-IR) spectrometry analysis

The sample was scanned by FT-IR spectrometry using PerkinElmer spectrophotometer (Los Angeles, CA). Briefly 2 mg of sample was mixed 200 mg Potassium bromide (KBr) (FT-IR grade) and pressed into a pellet and placed into the sample holder and FT-IR spectra were scanned in rang 4000–400 cm^{-1} in FTIR spectrometry at a resolution of 1 cm^{-1}.

2.7.1. Effect of parameters on controlling the size AgNPs

To study size control of AgNps we investigate effect of temperature and $AgNO_3$ concentration on size of AgNps, to achieve this purpose we used different concentrations of $AgNO_3$ (10^{-1}, 10^{-2} and 10^{-3} M), temperatures (10, 20, 40, 60, 80 °C). Biosynthesized AgNP size measurements were determined by TEM.

2.8. Statistical analysis

Origin professional eight (Microsoft, USA) software was used statistical Gaussian approximation to find full width at half maximum (FWHM) and calculation of One way Anova, P value < 0.05 is considered statistically significant.

3. Results and discussion

The pure colonies obtained and known as *R. stolonifer* supported the microscopic results. Addition of 100 ml of *R. stolonifer* mycelial aqueous extract to aqueous solution of silver nitrate at final concentration 1 mM, turned pale yellow color of *R. stolonifer* mycelial filtrate to reddish brown color within 48 h (Fig. 1). This result indicates the formation and deposition of silver AgNPs while original color of silver nitrate (negative control) remains unchanged. Usually, AgNPs formation is detected by color change observation of reaction medium from colorless to yellowness or dark brown (Karbasian et al., 2008). Color change of solution is due to excitation of surface Plasmon vibrations of AgNPs (Gericke and Pinches, 2006).

UV–Visible spectrometry showed optical absorption spectra of AgNPs ranging from 300 to 600 nm. The absorption spectra show one outstanding symmetric peak around 420 nm. That is as a result of surface plasmon resonance of AgNPs (Fig. 2). This spectroscopic pattern results from interactions of free electrons limited to tiny metallic spherical objects with episode electromagnetic wave. To study effect of time on AgNPs production, we measured UV–Vis spectra at different time, we found that absorbance at 420 nm increased with the incubation time of the silver nitrate with the mycelium extract. The statistical analysis showed a significant difference (P value = 0.001) in the production of AgNPs (Fig. 3) the highest production of AgNPs was after 48 h of incubations. UV-spectroscopy showed increased absorbance with time and AgNPs were synthesized by 24 h and there was almost no increase in absorbance after 48 h for the four tested *Aspergillus* species (Neveen and Khalil, 2013). An increase in intensity of the absorbance peak with time indicates the continued reduction of the silver ions and an increase in concentration of AgNPs (Birla et al., 2013). Electronic style of AgNPs is notably sensitive to their form and size, resulting in clear effects in its visible spectrum pattern. One of interesting criteria is increasing bandwidth of resonance with the decrease in the dimensions of the particles as a result of electron scattering induction at the surface. Resonance shifting and the variation of its bandwidth are important information for nanoparticles characterization. The presence of Plasmon band at 420 nm due to dipole plasmon resonance shows that the AgNPs have a spherical shape (Sathishkumar et al., 2009; Kannan et al., 2011). The full-width at half-maximum (FWHM) provide useful tool for determination size of nanoparticles and their distribution in the medium based on the concept of Brown et al. (Mock et al., 2002). In our study the FWHM of the AgNPs is 79.42 nm (Fig. 2). It's concluded that a FWHM of 79.42 nm is mostly an indication of a small size distribution. Thus, the synthesis of AgNPs using *R. stolonifer* is a promising and appropriate technique for preparation of uniform AgNPs with a small size distribution.

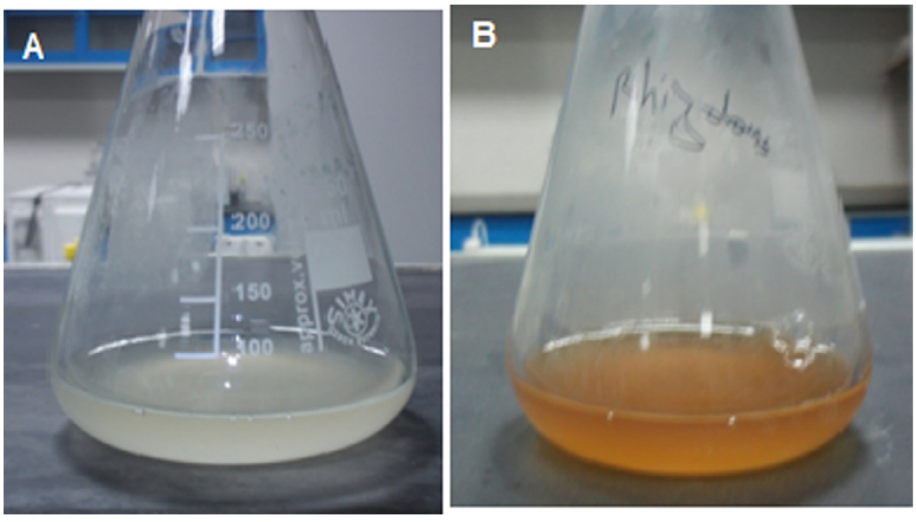

Figure 1 Visible observation of AgNPs biosynthesis. (A) ErlenMeyer flask with *R. stolonifer* mycelial filtrate after exposure to $AgNO_3$ solution (1 mM) for a few minutes (no color change), and (B) ErlenMeyer flask with *R. stolonifer* mycelial filtrate after exposure to $AgNO_3$ solution (1 mM) for 48 h (reddish-brown color).

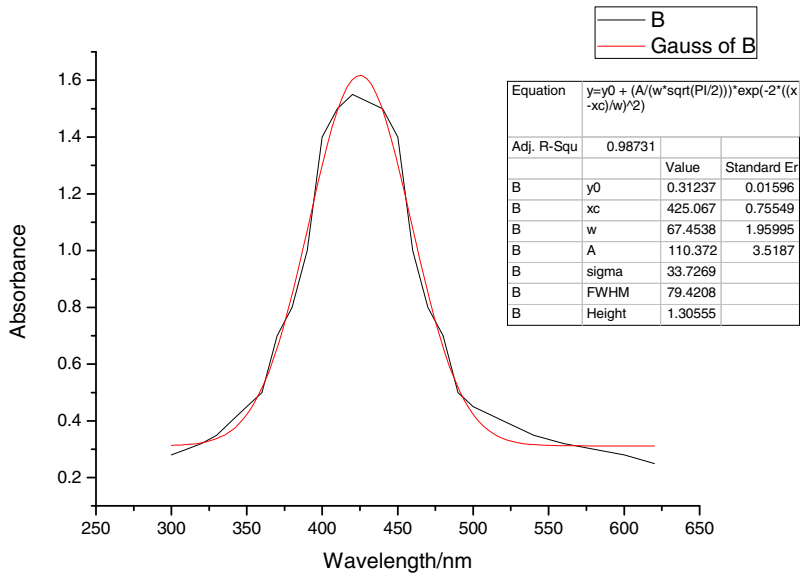

Figure 2 UV–vis spectra of prepared Ag NPs, B-optical absorption spectra and its Gauss of B. Inserted table show statistical Gaussian approximation was performed to find FWHM).

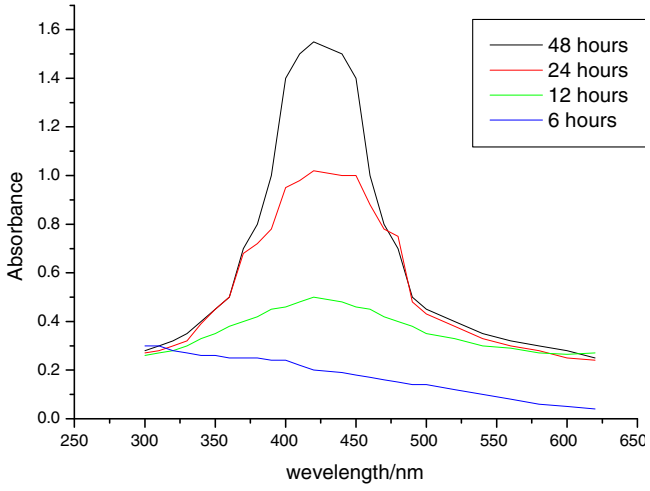

Figure 3 UV–visible absorption spectra of produced AgNPs using *Rhizopus stolonifer* mycelium extract at different incubation times, synthesis of SNPs is the function of time.

XRD analysis of the synthesized AgNPs showed three diffraction peaks at $2\Theta = 37.65°$, 44.85° and 64.89° that are corresponding to Bragg's reflections of the face-centered cubic (fcc) structure of metallic silver, (1 1 1), (2 0 0) and (2 2 0) respectively (Fig. 3). All diffraction peaks are in proper agreement with the quality value (JCPDS card No. 04-0783). This XRD line width is often used to estimate the dimensions of the particle by the Debye–Scherrer equation $d = 0.9\lambda/\beta \cos \Theta$, wherever d is the particle size, λ is the wavelength of X-ray radiation (1.5406 Å), β is the FWHM of the height (in radians) and 2Θ is the Bragg angle. The calculated average particle size was around 9.46 ± 2.64 nm.

TEM is considered a high resolution tool that gives actual information concerning particle size and shape (Jin et al., 2001; Sathishkumar et al., 2009). Recent HRTEM has the ability to image atoms directly in specimens at resolutions about 1 Å, smaller than inter-atomic space. This technique is very necessary for characterizing materials at a length scale from atoms to hundred nanometers. Fig. 4 shows HRTEM imaging of AgNPs. All AgNPs have a spherical form and diameter about 6.04 nm. Spherical form of prepared AgNPs highly agree with the fact given by (Brown et al., 2000), this confirms that surface plasmon peak around 420 nm indicate that the AgNPs have spherical form. The AgNPs were monodispersed and stable.

Fourier transform infrared spectrum indicted that mycelia aqueous extract of *R. stolonifer* contain active biomolecules which are responsible for biotransformation of silver ion to metallic AgNPs, that revealed distinct peak within the range of 3750–500 cm^{-1} (Fig. 4). The broad peak at 3500 cm^{-1} is resulting from strong stretching vibration of phenolic hydroxyl OH (Link and El-Sayed, 2000). The band at 2624 is due to an NH group from peptide linkage in the mycelia aqueous extract of *R. stolonifer* (Wang, 2000). The peak at 1684 is characteristic of amid group NHCO. Infrared (IR) analysis study has confirmed that carbonyl group resulted from amino acid residue and peptide protein can strongly bind to metal, so protein may act as capping protein of AgNPs which prevents agglomeration and stabilizes particles within the medium. This proof suggests that the biological molecules are responsible for biotransformation of silver ions to AgNPs and its stabilization in aqueous medium. It is a well known character of protein that it can bind to AgNPs through a free amine group and stabilization of AgNPs may be due to the surface bound protein (Gopinath et al., 2012). The peaks at 1426 and 1634 cm^{-1} are corresponding to carbonyl stretch vibrations in the amid linkages of proteins (Mubarakali et al., 2011). The carbonyl group from amino acid residues and peptides remains has strong capability to bind to silver (Gole et al., 2001). Also it is reported that proteins will bind to nanoparticles either through free amino or cysteine group in proteins (Basavaraja et al., 2008). The peaks at 1952, 1426 and 1684 cm^{-1} are correspond-

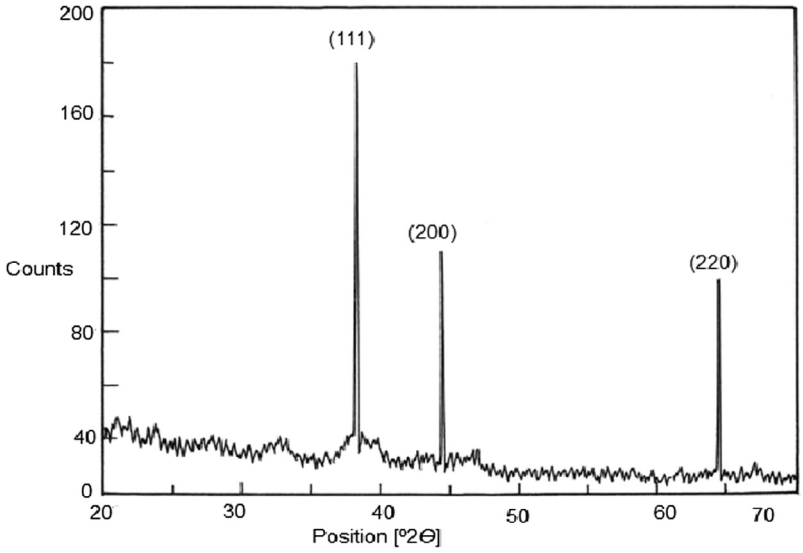

Figure 4 X-ray diffraction pattern of the AgNPs.

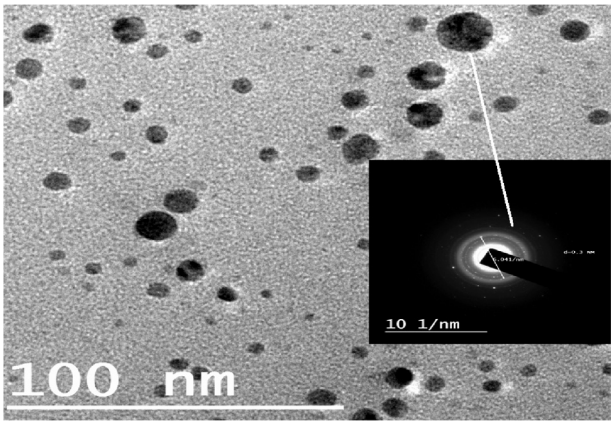

Figure 5 HRTEM pictures of the mono distributed spherical AgNPs (x = 100 nm) (inserted picture: selected area electron diffraction pattern).

ing AgNPs binding between oxygen from hydroxyl group and amid carbonyl groups of *R. stolonifer* mycelia extract (Mandal et al., 2005) (Fig. 5).

From FTIR results we conclude that the presence of protein in reaction medium provide reducing agent and coat covering for AgNPs known as capping proteins. Capping protein prevents agglomeration of AgNPs in the medium and responsible for forming high stable AgNPs. Similar results are obtained with bacteria (Kumar and Mamidyala, 2011) and Algae (Sudha et al., 2013). However polymers and surfactants were widely used as capping agent in preparation of AgNPs, protein capping provides advantage over polymer and surfactant as it is coast effective, safe, ecofriendly and does not need special conditions. Several harmful chemical by-products, metallic aerosol, irradiation, etc. are commonly produced during use of chemical and physical in AgNPs synthesis processes. These, along with the facts that these processes are expensive, time consuming, and typically done on small laboratory scale, render these methods less suitable for large-scale production (Mansoori, 2005; Sahu and Biswas, 2010). Another advantage of protein capping when compared to polymer and surfactant is it acts as the anchoring layer for drug or genetic materials to be transported into human cells (Hu et al., 2011). The presence of a nontoxic protein cap also increases uptake and retention inside human cells (Rodriguez et al., 2013). The presence of natural capping proteins eliminates the postproduction steps of capping which is necessary for most of applications of nanoparticles in the field of medicine (Chowdhury et al., 2014) (see Fig. 6).

Previous studies reported that size of AgNPs and micrometer scale Ag could be controlled by temperature or by molar ratio (Wang et al., 2010; Sun and Luo, 2005). In order to know how mycelium extracts control the size of AgNPs, we examined the effects of metal concentrations and temperature. Our findings showed no AgNPs was produced at 10 °C or at 80 °C this due to denaturation or inactivation of enzymes and active molecules which are involved in biogenesis of AgNPs either by a low or high temperature. Small monodispersed AgNPs with average size 2.86 ± 0.3 nm were produced at 40 °C (Fig. 7), Large AgNPs with average particle size 25.89 ± 3.8 and 48.43 ± 5.2 nm were produced at 20 °C and 60 °C respectively (Figs. 8 and 9). This increase in AgNPs size is due to low activity of enzymes involved in AgNPs biogenesis as a result of unsuitable temperature. Quite similar results were reported at a temperature (50 °C), most AgNPs were small. Further incubation at higher temperatures, the enzymes have denatured nature this lead to increase in particles size according to loss of enzyme activity (Sherif et al., 2015). Closed results were obtained by (Birla et al., 2013). At an increased temperature, the kinetic energy of the AgNPs in the solution also increases and collision frequency between the particles also rises resulting in a higher rate of agglomeration (Sarkar et al., 2007).

In order to investigate the effect of $AgNO_3$ concentration on size of AgNPs we applied different concentrations of $AgNO_3$ (10^{-1}, 10^{-2} and 10^{-3} M) and temperature was fixed at 40 °C. The smallest AgNP size (2.86 ± 0.3 nm) was

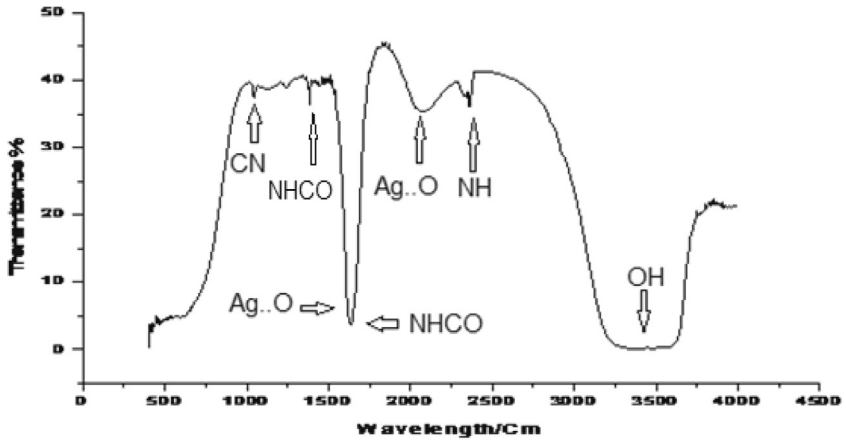

Figure 6 Fourier-transform infrared spectra of AgNPs biosynthesized by *R. stolonifer* after 48 h from biosynthesis reaction.

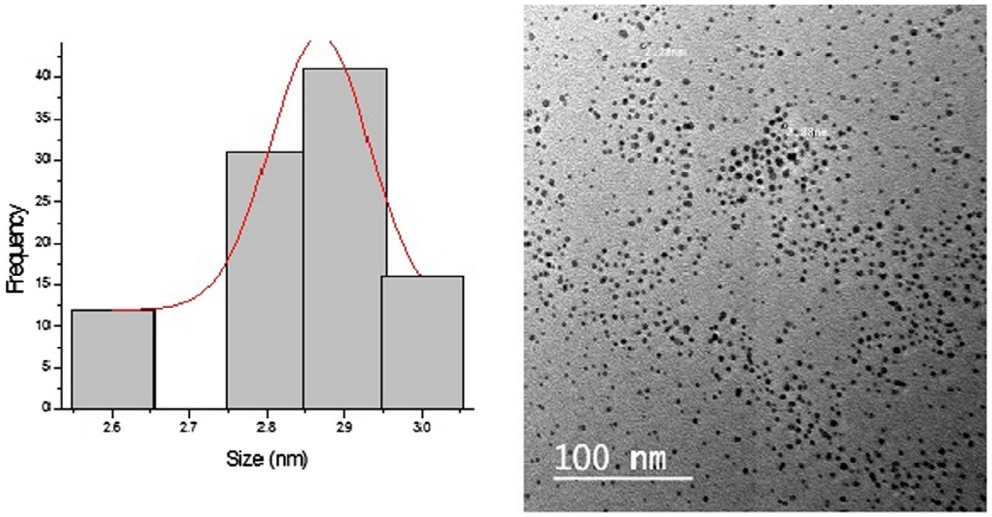

Figure 7 HRTEM image (x = 100 nm) and size distribution histogram of AgNPs prepared at 40 °C and 10^{-2} M $AgNO_3$.

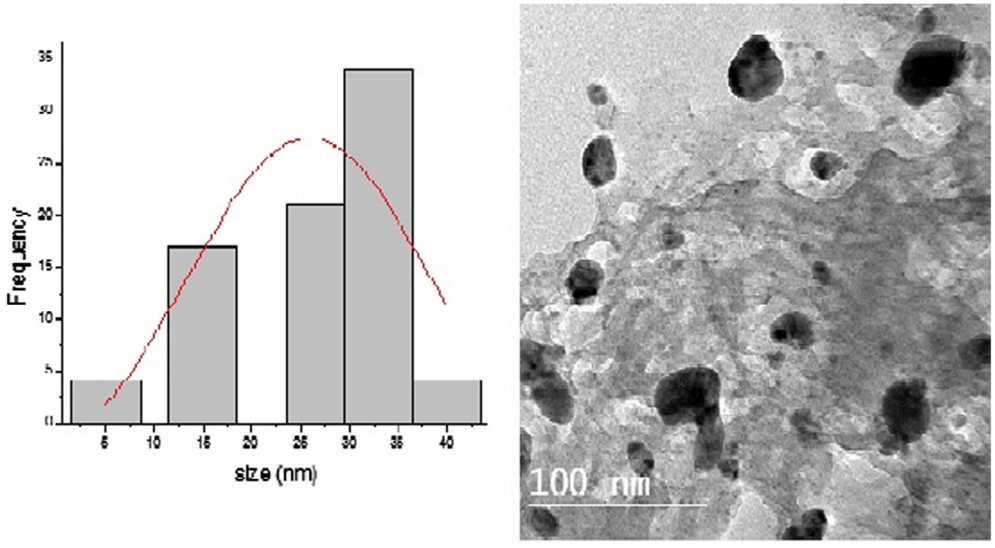

Figure 8 HRTEM image (x = 100 nm) and size distribution histogram of AgNPs prepared at 20 °C.

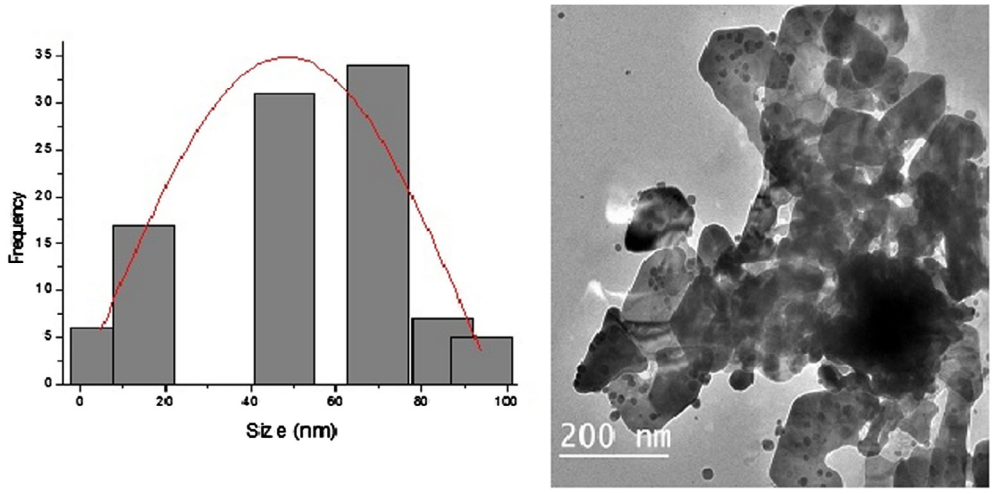

Figure 9 HRTEM image (x = 200 nm) and size distribution histogram of AgNPs prepared at 60 °C.

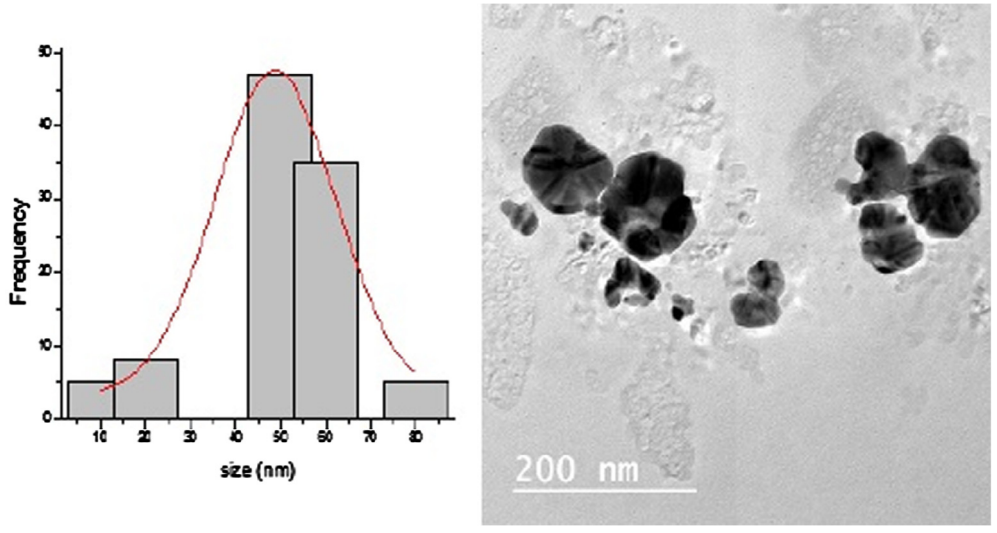

Figure 10 HRTEM image (x = 200 nm) and size distribution histogram of AgNPs prepared at a concentration 10^{-1} M of $AgNO_3$.

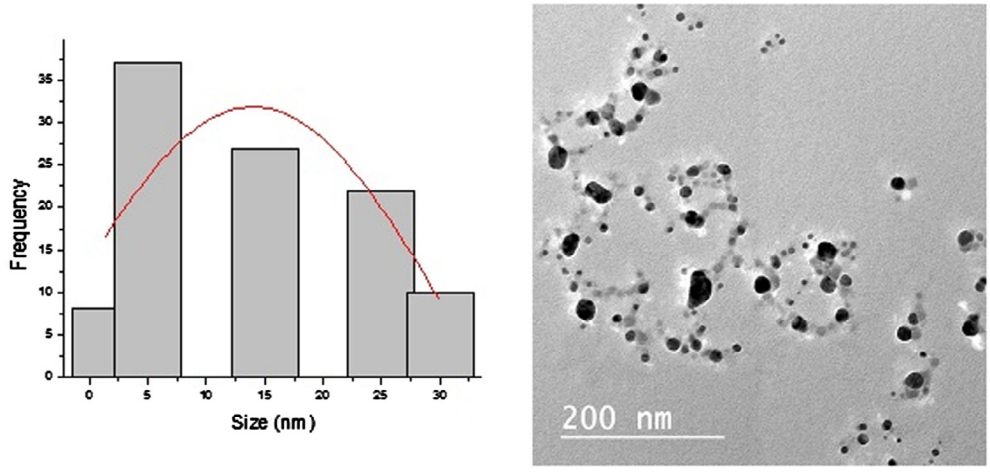

Figure 11 HRTEM image (x = 200 nm) and size distribution histogram of AgNPs prepared at a concentration 10^{-3} M of $AgNO_3$.

obtained at concentration 10^{-2} M of $AgNO_3$ (Fig. 7). Large AgNPs with average particle size 54.67 ± 4.1 and 14.23 ± 1.3 nm and were prepared at concentration 10^{-1}, 10^{-3} M of $AgNO_3$ respectively (Figs. 10 and 11). Usually, the optimum concentration of silver nitrate (1 mM) is used for the synthesis of $AgNO_3$ (Ahmad et al., 2003). Smallest AgNPs were obtained at 10^{-2} M of metal ion and excess addition of metal ions with concentration 10^{-1} M results in formation of very large particles exhibiting irregularly shaped that most of the cell enzymes were consumed by reduction of particles, demonstrating the high capacity of the cells for silver reduction (Sherif et al., 2015).

4. Conclusion

In the present study mono-dispersed AgNPs were prepared by mycelial aqueous extract of *R. stolonifer*. They have spherical form with an average size of 9.46 ± 2.64 nm. The AgNPs were characterized by UV–visible, XRD, TEM and FT-IR spectra. Biological synthesis of AgNPs using *R. stolonifer* is cheap, nonpolluting and safe technique and is a good alternative to chemical and physical methods. Our finding confirmed that mycelial aqueous extract of *R. stolonifer* could be a powerful tool for biosynthesis and stabilization of silver ion to AgNPs. However our results showed that temperature and metal ion concentration are playing an important role in AgNP size control; further studies are required to study kinetics of AgNPs reaction and effect of more parameters on size, geometry and morphology of AgNPs. These studies are important for controlling AgNPs in large scale production and production of high quality uniform AgNPs.

Acknowledgment

The authors extend their appreciation to the Deanship of Scientific Research at King Saud University for funding this work through research group No. (RG – 1435 – 060).

References

Ahmad, A., Mukherjee, P., Senapati, S., Mandal, D., Khan, M., Kumar, R., Sastry, M., 2003. Extracellular biosynthesis of silver nanoparticles using the fungus *Fusarium oxysporum*. Colloids Surf B. 28, 313–318.

Balaji, D., Basavaraja, S., Deshpande, R., Bedre, M., Prabhakara, B., Venkataraman, A., 2009. Extracellular biosynthesis of functionalized silver nanoparticles by strains of *Cladosporium cladosporioides* fungus. Colloids Surf. B 68, 88–92.

Balali, G.R., Neate, S.M., Scott, E.S., Whisson, D.L., Wicks, T.J., 1995. Anastomosis group and pathogenicity of isolates of *Rhizoctonia solani* from potato crops in South Australia. Plant Pathol. 44 (6), 1050–1057.

Basavaraj, U., Praveenkumar, N., Sabiha, T.S., Rupali, S., Samprita, B., 2012. Synthesis and characterization of silver nanoparticles. Int. J. Pharm. Bio Sci. 3, 10–14.

Basavaraja, S., Balaji, S., Lagashetty, K., Rajasab, H., Venkataraman, A., 2008. Extracellular biosynthesis of silver nanoparticles using the fungus *Fusarium semitectum*. Mater. Res. Bull. 43, 1164–1170.

Birla, S., Gaikwad, S., Gade, A., Rai, M., 2013. Rapid synthesis of silver nanoparticles from *Fusarium oxysporum* by optimizing physicocultural conditions. Sci. World J., 2013

Brown, R., Walter, G., Natan, M., 2000. Seeding of colloidal Au nanoparticles solution. 2. Improved control of particle size and shape. J. Chem. Mater. 12, 306–313.

Cho, K., Park, E., Osaka, T., Park, S., 2005. The study of antimicrobial activity and preservative effects of nanosilver ingredient. Electrochim. Acta 51, 956–960.

Chowdhury, S., Basu, A., Kundu, S., 2014. Green synthesis of protein capped silver nanoparticles from phytopathogenic fungus *Macrophomina phaseolina* (Tassi) Goid with antimicrobial properties against multidrug-resistant bacteria. Nanoscale Res. Lett. 9, 1–11.

Domsch, K.H., Gams, W., Anderson, T.H., 1993. Compendium of Soil Fungi. Academic Press, London, p. 860.

Gericke, M., Pinches, A., 2006. Microbial production of gold nanoparticles. Gold Bull. 39, 22–28.

Gole, A., Dash, C., Ramachandran, V., Sainkar, S., Mandale, A., Rao, M., Sastry, M., 2001. Pepsin-gold colloid conjugates: preparation, characterization, and enzymatic activity. Langmuir 17, 1674–1679.

Gopinath, V., Mubarak, D., Priyadarshini, S., Meera, P., Thajuddin, N., Velusamy, P., 2012. Biosynthesis of silver nanoparticles from *Tribulus terrestris* and its antimicrobial activity: a novel biological approach. Colloids Surf. B Biointerfaces, 69–74.

Govindaraju, K., Tamilselvan, S., kiruthiga, V., Singaravelu, G., 2010. Biogenic silver nanoparticles by *Solanum torvum* and their promising antimicrobial activity. J. Biopest. 1, 394–399.

Hu, J., Zhang, L., Aryal, S., Cheung, C., Fang, H., Zhang, L., 2011. Erythrocyte membrane-camouflaged polymeric nanoparticles as a biomimetic delivery platform. PNAS 108, 10980–10985.

Jin, R., Cao, Y., Mirkin, C.A., Kelly, K., Schatz, G., Zheng, J., 2001. Photoinduced conversion of silver nanospheres to nanoprisms. Science 30, 1901–1903.

Kalishwaralal, K., Deepak, V., Ramkumarpandian, S., Nellaiah, H., Sangiliyandi, G., 2008. Extracellular biosynthesis of silver nanoparticles by the culture supernatant of *Bacillus licheniformis*. Mater. Lett. 62, 4411–4413.

Kannan, N., Mukunthan, K.S., Balaji, S., 2011. A comparative study of morphology, reactivity and stability of synthesized silver nanoparticles using *Bacillus subtilis* and *Catharanthus roseus*. Colloids Surf. B. Biointerfaces 86, 378–383.

Karbasian, M., Atyabim, S., Siyadat, S., Momen, S., Norouzian, D., 2008. Optimizing nanosilver formation by *Fusarium oxysporum* PTCC 5115 employing response methodology. Am. J. Agric. Biol. 3, 433–437.

Kim, T., Feng, L., Kim, J., Wang, H., Chen, G., 1998. Antimicrobial effects of metal ions (Ag?, Cu2+?, Zn2+?) in hydroxyapatite. J. Mater. Sci. Mater. Med. 9, 129–134.

Kumar, C.G., Mamidyala, S.K., 2011. Extracellular synthesis of silver nanoparticles using culture supernatant of *Pseudomonas aeruginosa*. Colloids Surf. B 84, 462–466.

Link, S., El-Sayed, M., 2000. Shape and size dependence of radiative, nonradiative, and photothermal properties of gold nanocrystals. Int. Rev. Phys. Chem. 19, 409.

Mandal, S., Phadtare, S., Sastry, M., 2005. Interfacing biology with nanoparticle. Curr. Appl. Phys. 5, 118–127.

Mann, S., 1996. Biomimetic Materials Chemistry. VCH Publishers, New York.

Mansoori, G.A., 2005. Principles of nanotechnology: molecular-based study of condensed matter in small systems. World Scientific.

Mock, J., Barbic, M., Smith, R., Schultz, D., Schultz, S., 2002. Shape effects in plasmon resonance of individual colloidal silver nanoparticles. J. Chem. Phys. 116, 6755–6759.

Mubarakali, D., Thajuddin, N., Jeganathan, K., Gunasekaran, M., 2011. Plant extract mediated synthesis of silver and gold nanoparticles and its antibacterial activity against clinically isolated pathogens. Colloids Surf. B. Biointerfaces 85, 360–365.

Mukherjee, P., Roy, M., Mandal, B., 2008. Green synthesis of highly stabilized nanocrystalline silver particles by a nonpathogenic and agriculturally important fungus *T. asperellum*. J. Nanotechnol. 19, 7.

Neveen, M., Khalil, 2013. Biogenic silver nanoparticles by *Aspergillus terreus* as a powerful nanoweapon against *Aspergillus fumigatus*. Afr. J. Microbiol. Res. 7, 5645–5651.

Qin, X., Lu, W., Luo, Y., Chang, G., Sun, X., 2011. Preparation of Ag nanoparticle-decorated polypyrrole colloids and their application for H_2O_2 detection. Electrochem. Commun. 13 (8), 785–787.

Rai, M., Yadav, A., Gade, A., 2009. Silver nanoparticles as a new generation of antimicrobials. Biotechnol. Adv. 27, 76–83.

Rao, C., Kulkarni, G., Thomas, P., Edwards, P., 2000. Metal nanoparticles and their assemblies. Chem. Soc. Rev. 29, 27–35.

Rodriguez, L., Harada, T., Christian, A., Pantano, A., Tsai, K., Discher, E., 2013. Minimal "Self" peptides that inhibit phagocytic clearance and enhance delivery of nanoparticles. Science 339, 971–975.

Sahu, M., Biswas, P., 2010. Size distributions of aerosols in an indoor environment with engineered nanoparticle synthesis reactors operating under different scenarios. J. Nanopart. Res. 12, 1055–1064.

Sarkar, S., Jana, D., Samanta, K., Mostafa, G., 2007. Facile synthesis of silver nano particles with highly efficient antimicrobial property. Polyhedron 26, 4419–4426.

Sathishkumar, M., Sneha, K., Won, S., Cho, C., Kim, S., Yun, Y., 2009. *Cinnamon zeylanicum* bark extract and powder mediated green synthesis of nano-crystalline silver particles and its bactericidal activity. Colloids Surf. B. Biointerfaces 73, 332–338.

Shahverdi, A., Fakhimi, A., Shahverdi, H., Minaian, S., 2007. Synthesis and effect of silver nanoparticles on the antibacterial activity of different antibiotics against *Staphylococcus aureus* and *Escherichia coli*. Nanomed. Nanotechnol. Biol. Med. 3, 168–171.

Sherif, H., Taher, S., Hend, A., 2015. Biosynthesis of size controlled silver nanoparticles by *Fusarium oxysporum*, their antibacterial and antitumor activities. Beni-Suef Univ. J. Basic Appl. Sci. 4, 225–231.

Simkiss, K., Wilbur, K., 1989. Biomineralization, Cell Biology and Mineral Deposition. Academic Press, New York, p. 337.

Sudha, S., Rajamanickam, K., Rengaramanujam, J., 2013. Microalgae mediated synthesis of silver nanoparticles and their antibacterial activity against pathogenic bacteria. Ind. J. Exp. Biol. 51, 393–399.

Sun, X., Luo, Y., 2005. Preparation and size control of silver nanoparticles by a thermal method. Mater. Lett. 59, 3847–3850.

Wang, L., Li, H., Tian, J., Sun, X., 2010. Monodisperse, micrometer-scale, highly crystalline, nanotextured Ag dendrites: rapid, large-scale, wet-chemical synthesis and their application as SERS substrates. ACS Appl. Mater. Interfaces 2, 2987–2991.

Wang, Z., 2000. Transmission electron microscopy of shape-controlled nanocrystals and their assemblies. J. Phys. Chem. B 104, 1153–1175.

Zhang, Y., Wang, L., Tian, J., Li, H., Luo, Y., Sun, X., 2011. Ag@ poly (m-phenylenediamine) core–shell nanoparticles for highly selective, multiplex nucleic acid detection. Langmuir 27, 2170–2175.

Zhong-jie, J., Chun-yan, L., Lu-wi, S., 2005. Catalytic properties of silver nanoparticles supported on silica spheres. J. Phys. Chem. B 109, 1730–1735.